

Using a triple-quadrupole mass spectrometer in accurate mass mode and an ion correlation program to identify compounds[†]

Andrew H. Grange^{1*}, Witold Winnik², Patrick L. Ferguson¹ and G. Wayne Sovocool¹

¹U.S. EPA, ORD, NERL, Environmental Sciences Division, PO Box 93478, Las Vegas, NV 89193-3478, USA

²U.S. EPA, ORD, NHEERL, Environmental Carcinogenesis Division, Research Triangle Park, NC 27111, USA

Received 28 April 2005; Revised 19 July 2005; Accepted 21 July 2005

Atomic masses and isotopic abundances are independent and complementary properties for discriminating among ion compositions. The number of possible ion compositions is greatly reduced by accurately measuring exact masses of monoisotopic ions and the relative isotopic abundances (RIAs) of the ions greater in mass by +1 Da and +2 Da. When both properties are measured, a mass error limit of 6–10 mDa (<31 ppm at 320 Da) and an RIA error limit of 10% are generally adequate for determining unique ion compositions for precursor and fragment ions produced from small molecules (less than 320 Da in this study). 'Inherent interferences', i.e., mass peaks seen in the product ion mass spectrum of the monoisotopic [M+H]⁺ ion of an analyte that are -2, -1, +1, or +2 Da different in mass from monoisotopic fragment ion masses, distort measured RIAs. This problem is overcome using an ion correlation program to compare the numbers of atoms of each element in a precursor ion to the sum of those in each fragment ion and its corresponding neutral loss. Synergy occurs when accurate measurement of only one pair of +1 Da and +2 Da RIAs for the precursor ion or a fragment ion rejects all but one possible ion composition for that ion, thereby indirectly rejecting all but one fragment ion-neutral loss combination for other exact masses. A triple-quadrupole mass spectrometer with accurate mass capability, using atmospheric pressure chemical ionization (APCI), was used to measure masses and RIAs of precursor and fragment ions. Nine chemicals were investigated as simulated unknowns. Mass accuracy and RIA accuracy were sufficient to determine unique compositions for all precursor ions and all but two of 40 fragment ions, and the two corresponding neutral losses. Interrogation of the chemical literature provided between one and three possible compounds for each of the nine analytes. This approach for identifying compounds compensates for the lack of commercial ESI and APCI mass spectral libraries, which precludes making tentative identifications based on spectral matches. Published in 2005 by John Wiley & Sons, Ltd.

Each year 2800 high-volume production chemicals (those with annual production of at least 10⁶ lbs)¹ and 87 000 commercially produced chemicals,² along with their synthetic precursors, byproducts, transformation products, and metabolites, ultimately enter waste streams. The ability to identify compounds not targeted by routine analytical methods is important for assessing risks posed to aquatic ecosystems and to human health. In addition, sabotage agents not included on target lists of analytical methods could pose identification problems.

*Correspondence to: A. H. Grange, U.S. EPA, ORD, NERL, Environmental Sciences Division, PO Box 93478, Las Vegas, NV 89193-3478, USA.

E-mail: grange.andrew@epa.gov

[†]Although this work was reviewed by the EPA and approved for publication, it may not necessarily reflect official Agency policy.

Mass spectrometry (MS) has been used extensively for structural elucidation of chemical compounds. Two independent physical properties distinguish among the MS ion compositions possible for a given nominal mass: the exact masses of ions and the relative isotopic abundances (RIAs) of ions greater in mass by 1 Da and 2 Da (in this work, these higher mass ions will refer to [M+H+1]⁺ and [M+H+2]⁺ ions) that arise from the presence of atoms of heavier stable isotopes of elements, e.g., ¹³C, ²H, ¹⁵N, ¹⁷O, ¹⁸O, ³³S, ³⁴S, ³⁷Cl, and ⁸¹Br. Ion composition elucidation (ICE) is a high-resolution MS technique³ that determines both exact masses and RIAs by acquiring selected ion recording (or multiple ion detection) data on a chromatographic elution time scale. Simultaneous measurement of the exact masses and RIAs of the +1 Da and +2 Da isotopic profiles increases by four-fold the upper mass limit of ions for which a unique elemental composition can be determined.⁴ Over the last decade, ICE

has been shown in this laboratory to be a powerful analytical technique for characterization and identification of compounds from Superfund sites,⁵ municipal wells,⁶ lakes,⁷ streams,⁸ and sewage treatment effluents⁹ using gas chromatography/high-resolution mass spectrometry (GC/HRMS).

Despite its demonstrated utility, two disadvantages have discouraged adoption of ICE by other laboratories. First, until recently, a double-focusing mass spectrometer has been required, both to measure accurate masses and to provide a wide linear dynamic range to measure accurate RIAs.¹⁰ Flexible custom software unique to each data system, rather than prepackaged procedures, is required to automatically acquire and process the data needed to determine exact masses and RIAs of ions. The currently manufactured instruments cannot conveniently acquire and process the necessary data, because the instrument makers no longer provide a macro language and command line from which users can execute lists of commands stored as ASCII files.

Second, the technique has been time-consuming and labor-intensive. A series of three experiments employing a successive approximation approach is usually required to determine the composition of an apparent molecular ion.¹⁰ Thereafter, two experiments are required to determine the composition of each fragment ion. In practice, fragment ion compositions are determined only for compounds not found in NIST¹¹ or Wiley¹² mass spectral libraries, or when mass interferences prevent determination of unique compositions for apparent molecular ions.

For ICE to become practical and more frequently used, it must be adapted to a user-friendly bench-top instrument, require fewer experiments, and use a robust data system software package to acquire all necessary data and to report lists of exact masses and RIAs.

In addition to magnetic sector instruments, orthogonal-acceleration time-of-flight (TOF) mass spectrometers have been used to obtain masses accurate to within 10 ppm^{13–17} or 5 ppm.^{18–21} However, to rival the capability of double-focusing mass spectrometers for determining ion compositions,¹⁰ a mass spectrometer must also provide RIAs of ions with greater accuracy than has been demonstrated in the past with these instruments, which provided limited dynamic ranges of between 50 and 200.^{13,16,21}

As shown in this work, a modern triple-quadrupole mass spectrometer, with a dynamic range of 10^5 , is able to measure masses with 10 mDa accuracy or RIAs with 10% accuracy for both the precursor ion and fragment ions during the same experiment. These tolerances are demonstrated here to be sufficient for identifying compounds using ICE. A utility-based definition of 'exact mass' is used in this paper. Although double-focusing and Fourier transform ion cyclotron resonance (FTICR) mass spectrometers can routinely measure exact masses to within 2 ppm or less, the term 'exact mass' is used in this paper to describe masses accurate to within 10 mDa. Ion masses accurate within this error limit are still useful for distinguishing among elemental compositions of ions possible based on their nominal masses.

In GC/MS studies many environmental 'unknowns' have been found in the mass spectral libraries, and ICE has provided confirmatory evidence for such tentative identifica-

tions. ICE has also provided the correct library match when multiple matches with multiple ion compositions for the highest-mass monoisotopic ion were found.²² Until now, ICE has seldom been used with liquid sample introduction^{23,24} but, because there are no commercial mass spectral libraries for electrospray chemical ionization (ESI) or atmospheric pressure chemical ionization (APCI), the ICE technique is likely to become essential in such analyses. To use liquid chromatography/mass spectrometry (LC/MS) for compound identification, determination of ion compositions is mandatory for hypothesizing compound identities prior to the confirmation of the hypothesis by LC/MS/MS analysis of authentic standards.

This work employed a modern triple-quadrupole instrument with APCI to evaluate whether or not the compositions of the precursor ion, fragment ions, and neutral losses from nine test compounds could be determined simply and efficiently, and if the compounds could be identified from these compositions.

EXPERIMENTAL

Standards

Thirteen standards were used as simulated unidentified compounds or calibrants: 2-aminobiphenyl (97%), phenazine (98%), 2-(methylthio)benzothiazole (97%), *N,N*-diethyl-3-methylbenzamide (97%), *N*-butylbenzenesulfonamide (99%), *N*-(3-chloro)-2,2'-iminodiethanol (98%), tris(2-chloroethyl)phosphate (97%), chlorpromazine hydrochloride (98%), *m*-anisidine (97%), 3-aminofluoranthene (97%), 4-aminopyridine (99+%), and sulfamerazine (98+%) were from Aldrich (Milwaukee, WI, USA), and pseudoephedrine was obtained from a cold remedy tablet.

HPLC

A Thermo Finnigan (San Jose, CA, USA) Surveyor[®] MS pump was used with a Zorbax[®] (Agilent, Foster City, CA, USA) RX-C18, 5 μ m particle, 2.1 mm \times 150 mm high-performance liquid chromatography (HPLC) column. A Thermo Finnigan Surveyor[®] autosampler made 10- μ L injections of a 1:1 methanol/water solution containing 1% acetic acid (glacial, reagent, ACS, VWR, PA, USA) and each of the nine surrogate unknowns present at 1 ng/ μ L. The two solvents, A and B, were respectively 2:98 and 98:2 methanol (high purity solvent; Burdick & Jackson, Muskegon, MI, USA)/water (Nanopure, Barnsted/Thermodyne, Dubuque, IA, USA), both with 0.2% acetic acid. The two-step linear solvent gradient (300 μ L/min) was: 100% A for 1 min, ramp to 70:30 A/B at 1.1 min, ramp to 40:60 A/B at 5 min, ramp to 30:70 A/B at 14 min, return to 100% A at 14.1 min, and maintain 100% A to 16 min. The mass calibration solution, infused at 5–15 μ L/min, joined the HPLC eluent through an LC mixing tee placed before the APCI source.

Mass spectrometry

The HPLC system was interfaced to a Thermo Finnigan TSQ Quantum Ultra AM[®] triple-quadrupole mass spectrometer (AM3QMS). The following APCI source settings were used: discharge current, 11 μ A; sheath gas pressure, 30 psi; vaporizer temperature, 400°C; and capillary temperature, 200°C.

The short transition times required by the AM3QMS to establish different scan parameters permitted monitoring of multiple target ions during the elution of each LC peak. Four scan methods were used in this study: full scanning using Q3 to determine retention times, product ion scanning at different collision-induced dissociation (CID) voltages to select fragment ions for further study, selected reaction monitoring (SRM) with internal mass calibration to measure exact masses of monoisotopic precursor and fragment ions, and SRM to measure RIAs of precursor and fragment ions. The mass resolution used in Q1 and Q3 depended on the kind of data to be obtained.

Full scans

Either Q1 or Q3 can be used for full spectral scanning. Q3 was scanned from m/z 50–450 Da with a mass peak width of 0.7 Da (FWHM, full width at half maximum) and a scan time of 0.5 s. The HPLC gradient was optimized based on viewing full scans to achieve separation of the analytes.

Product ion scans

Product ion scan ranges were from m/z 50 to a m/z value 8–20 Th greater than that of each precursor ion, with Q1 and Q3 peak widths (FWHM) of 0.7 Da. The scan time was 0.5 s, the Ar pressure in Q2 was 2 mTorr, and CID voltages of –12, –24, and –36 V were applied sequentially, changing to the next CID voltage after each scan. Only monoisotopic ions were passed by Q1 into the CID region to provide only monoisotopic fragment ions for analysis by Q3. The product ion spectra are displayed in Fig. 1.

Fragment ions that provided large ion abundances, and for which no neighboring ions within a ± 2 Da range were evident, were preferred for further investigation but were not always available. The ions labeled with a larger font in Fig. 1 at one of the CID voltages were investigated using that CID voltage. The voltage chosen for a fragment ion provided the lowest relative abundances of neighboring ions, or the largest ion abundance for the target ion if neighboring ion abundances were not significant.

Exact mass measurements

Exact mass measurements employed SRM across 1-Da mass ranges for (a) an analyte $[M+H]^+$ ion, (b) between two and six analyte fragment ions, and (c) between three and six calibrant $[M+H]^+$ ions used for internal mass calibration, using a Q1 FWHM of 0.7 Da and a Q3 FWHM of 0.1 Da, and CID voltages of –10, –12, –24, or –36 V, depending on the ion, 2 mTorr of argon collision gas in Q2, and a scan time of 0.05 s/ion. A mixture of six compounds provided $[M+H]^+$ calibration ion peaks at m/z 95.0604 (4-aminopyridine, $C_5H_7N_2^+$), 124.0757 (m-anisidine, $C_7H_{10}NO^+$), 166.1226 (pseudoephedrine, $C_{10}H_{16}NO^+$), 218.0964 (3-aminofluoranthene, $C_{16}H_{12}N^+$), 265.0754 (sulfamerazine, $C_{11}H_{13}N_4O_2S^+$), and 319.1030 (chlorpromazine, $C_{17}H_{20}N_2S^+$) for the nine analytes. For all calculations of ion mass, the mass of the electron, 0.00055 Da, was subtracted from the sums of the ions' atomic masses.

Equal volumes of 10 ng/ μ L solutions were combined; for compounds providing low ion abundances, additional volumes were added until all six ion abundances were within a factor of three of each other. Two of the calibrant

compounds were also used as surrogate unknowns: the exact masses of their precursor ions (m/z 166 and 319) were determined using external calibration.

As each analyte eluted into the APCI source, the precursor ion, fragment ions, and mass calibration ions that most closely bracketed the masses of the precursor ion and fragment ions under study, were selected sequentially by Q1 with a peak width of 0.7 Da. For each ion selected by Q1, a single 1-Da wide mass window was scanned by Q3 about the precursor, fragment, or calibrant ion mass, using a profile width at half maximum of 0.1 Da to ensure the entire profile was scanned. Profile shape stability in Q3 at different CID voltages was enhanced by using a relatively high Ar pressure of 2 mTorr. The CID voltage was –10 V for the $[M+H]^+$ calibration ions and –12 V for the $[M+H]^+$ analyte ions to minimize fragmentation. The fragment ions were generated from the $[M+H]^+$ ions using CID voltages of –12, –24, or –36 V, as indicated in Fig. 1.

Each of between 6 and 12 ions were scanned over 1-Da mass windows in Q3, depending on the number of fragment ions and calibration ions viewed for each analyte. The total cycle time for the 6–12 ions was between 0.23 and 0.44 s, respectively. The exact mass of each ion was measured from between 29 and 70 cycle averages depending on the chromatographic peak width at 20% of the maximum abundance above the baseline (8–21 s). The average exact masses of the analyte ions were corrected by the linearly interpolated error in the calibration masses that bracketed each one of them. Triplicate exact mass measurements were made for the nine precursor ions and 31 fragment ions listed in Table 1.

Relative isotopic abundance measurements

RIAs of analyte ions were measured using SRM mode across 1-Da mass ranges with a Q1 peak width of 10 Da and a Q3 peak width of 0.5 Da, using CID voltages of –12, –24, or –36 V, 2 mTorr of Ar in Q2, and a scan time of 0.05 s/ion. As illustrated in Fig. 1, monoisotopic product ions were observed when only the monoisotopic precursor ion was selected by Q1. To measure RIAs, all of the monoisotopic, +1 Da, and +2 Da ions from the precursor ion must enter Q2 for fragmentation, and for this reason the Q1 mass window was set to 10 Da with the +1 mass peak as the center of the Q1 isolation window. Each of the monoisotopic and multi-isotopic +1 Da and +2 Da mass peaks profiles for the precursor or fragment ion was scanned across 1 Da in the SRM mode with the Q3 resolution set to 0.5 Da to ensure none of the profiles was missed. The ratios of the areas under the appropriate chromatographic peaks (e.g., areas for m/z 167/166 and 168/166), multiplied by 100%, provided the RIAs (%1 RIA and %2 RIA). Three ions for each of three analytes (nine in all) were investigated for each injection. The presence of the accurate mass calibrant ions was not necessary for RIA measurements. Triplicate RIA measurements were made for the ions listed in Table 1. These four scan modes were used to study nine standards that provided adequate APCI signals, which served as simulated unknowns.

Prior to exact mass measurements, the 'Hi Res' and 'AM Calib' instrumental procedures were performed for the six $[M+H]^+$ calibrant ions for Q3. Then manual adjustment of

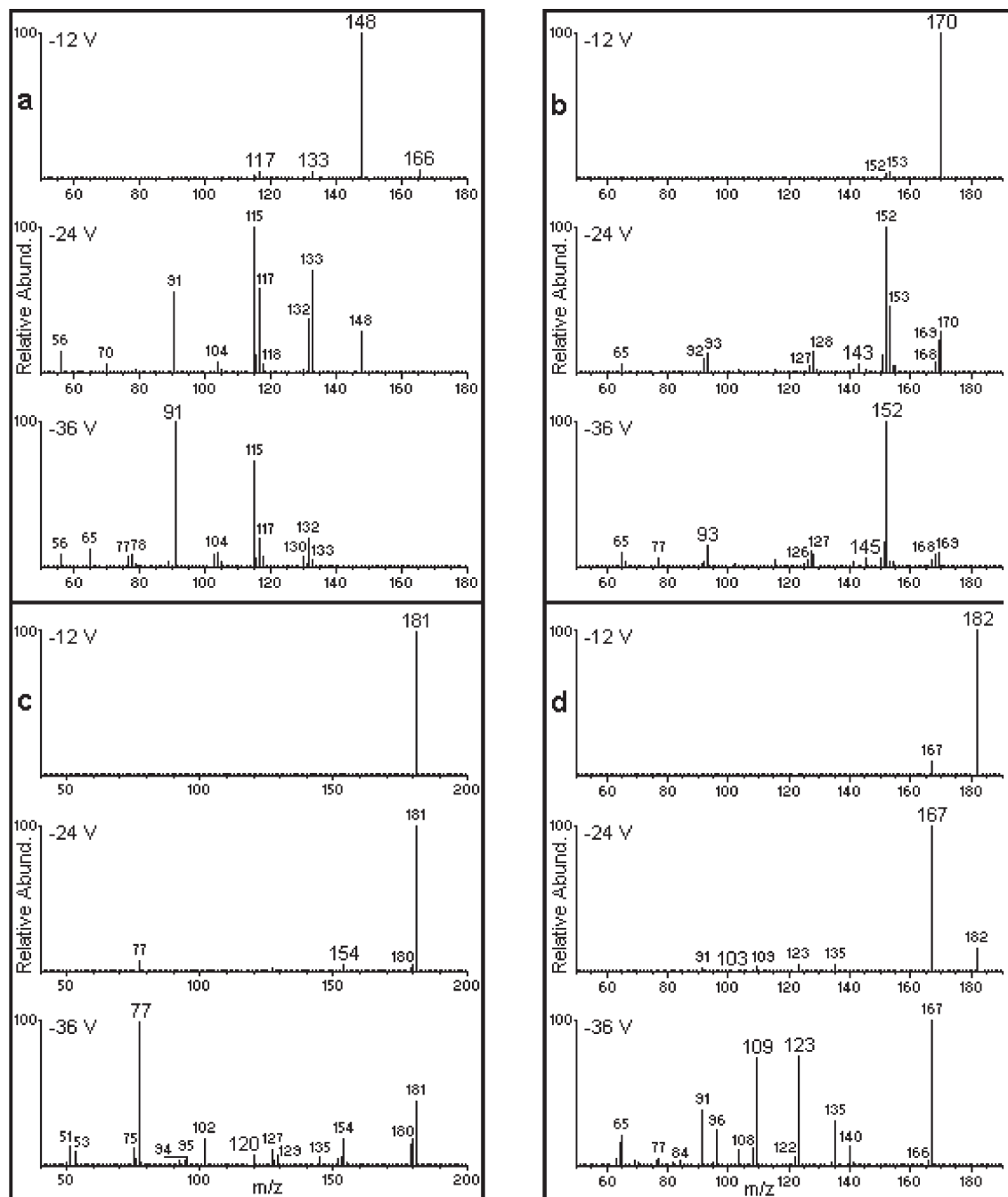


Figure 1. Monoisotopic product ion scans for nine 'simulated' unknowns: (a) pseudoephedrine, (b) 2-aminobiphenyl, (c) phenazine, (d) 2-(methylthio)benzothiazole, (e) *N,N*-diethyl-3-methylbenzamide, (f) *N*-butylbenzenesulfonamide, (g) *N*-(3-chloro)-2,2'-iminodiethanol, (h) tris(2-chloroethyl)phosphate, and (i) chlorpromazine. The analytes were separated by HPLC, and analyzed by MS/MS of the monoisotopic $[M+H]^+$ ions using CID voltages of -12 , -24 , and -36 V and 2 mTorr of Ar in Q2. The Q1 and Q2 profile widths were 0.7 Da (FWHM). Ions were investigated at the CID voltage for which the font for their nominal mass label is enlarged. (Continued over next two pages.)

various lens potentials was performed to fine-tune the Q3 profile width to 0.1 Da at half height for each of these ions. For RIA measurements, only the 'Auto Tune & Calib' and 'Mass Calib' procedures required for low mass resolution work were run for both Q1 and Q3.

RESULTS AND DISCUSSION

Complementarity of exact masses and RIAs

Historically, exact masses of monoisotopic ions have been measured to limit the number of possible compositions for

ions in a mass spectrum. However, the value of the RIAs for discriminating among the possible compositions has been underutilized. For example, the RIA of the +1 Da peak is often used to estimate the number of ^{13}C atoms in an ion. Likewise, the RIA of the +2 Da peak has provided the number of atoms of ^{37}Cl , ^{81}Br , and, in some cases, ^{34}S , while unusually small +1 Da and +2 Da RIAs suggest the presence of other common monoisotopic atoms which include I, As, or multiple atoms of F in addition to the very common P. In this work accurate measurements of RIAs, followed by their

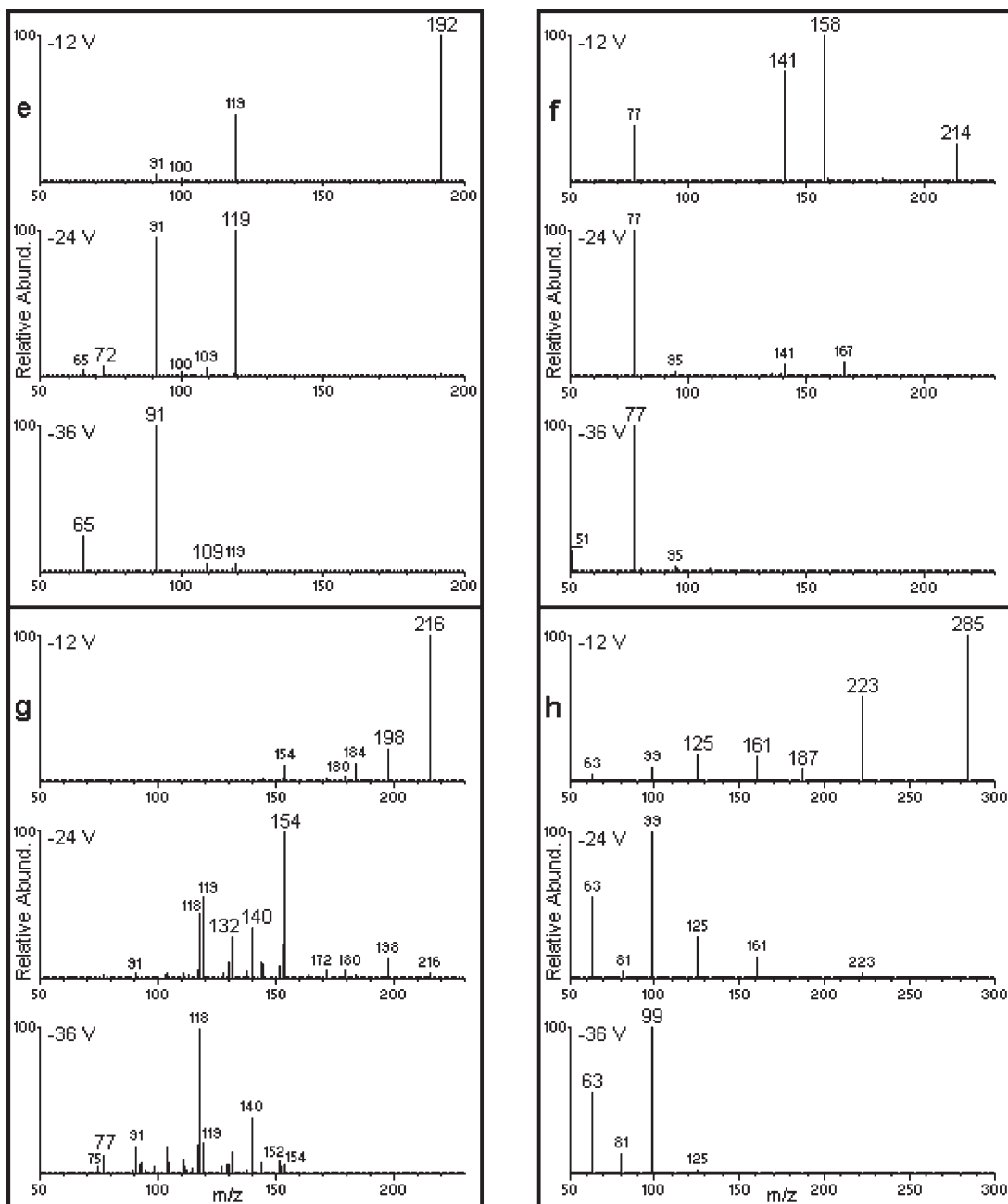


Figure 1. Continued.

automated comparison to RIA values calculated for all elemental compositions that were consistent with an ion's exact mass, were used to take fuller advantage of the discriminating power of RIAs.

Figure 2 demonstrates that use of the exact mass of the monoisotopic ion in conjunction with RIAs to discriminate among compositions is much more effective than using either property alone. A mass error limit of 7 mDa for a measured average exact mass of 391.0969 Da, together with the assumption that at least one-third of the mass was due to C atoms, yielded 172 possible compositions based on the allowed presence of C, H, Cl, N, O, P, and S atoms (Fig. 2(a)). Even with reduction of the mass error limit to 0.32 mDa (1 ppm) seven compositions were still possible (not shown). Similarly, by considering only the measured average

RIAs of 19.92% and 37.27% with an error limit of 10% of their values, 154 possible compositions were obtained (Fig. 2(b)). In contrast, consideration of the exact masses and RIAs simultaneously, with the 7 mDa and 10% error limits, yielded only the seven possible compositions shown in the bottom table of this figure (Fig. 2(c)).

The partial profile data acquired previously using a double-focusing mass spectrometer³ provided exact masses for the monoisotopic and multi-isotopic +1 Da and +2 Da mass peaks, and the RIAs, for the ion under scrutiny. However, even with mass error limits of 6 ppm, the discriminating power of the exact masses of the +1 Da and +2 Da profiles was less than that of the RIAs with an error limit of about 10% of the RIA values.¹⁰ While the exact masses of the +1 Da and +2 Da profiles provided supplemental data

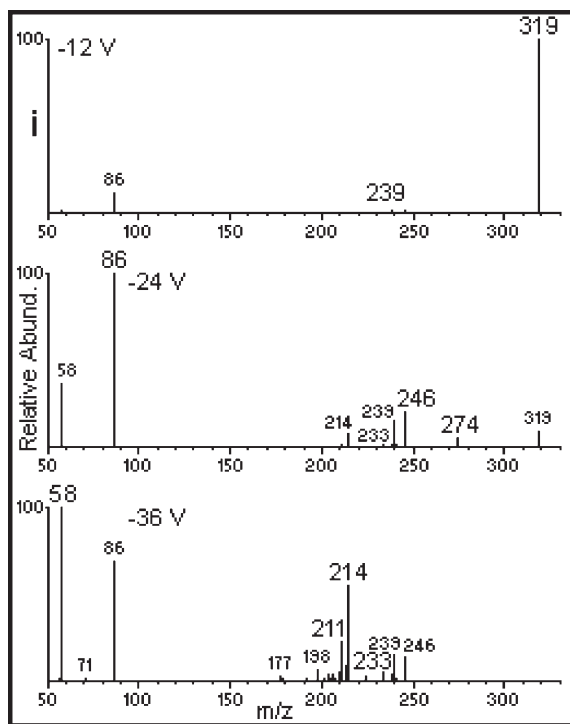


Figure 1. Continued

for confirming ion compositions, they were seldom essential to their determination. For this reason, and also because mass interferences are more likely to distort exact mass values obtained at lower mass resolving power for the less abundant +1 Da and +2 Da analyte profiles, only the exact masses of monoisotopic ions were measured in this study.

Complementarity of the precursor ion and its fragment ions and corresponding neutral losses

Figure 3 demonstrates the exponential increase in the number of possible ion compositions with increasing ion mass based on a 7-mDa mass error limit for the elements C, H, Cl, N, O, P, and S. The number of atoms considered for each element ranged from 0 to the largest integer less than or equal to the M/AM ratio, where M is the mass entered and AM the atomic mass of the element. A composition generator¹⁰ calculated that 1654 compositions were theoretically possible for a m/z 400.0000 ion. The number of possible compositions was dramatically reduced to 112 for a m/z 200.0000 fragment ion or neutral loss. Determination of the unique composition of a fragment ion or a neutral loss requires less stringent error limits than for the precursor ion. After the composition of a fragment ion or neutral loss has been subtracted from the precursor ion, the remaining atoms correspond to a smaller mass for which fewer compositions are possible. For instance, only one composition, $C_{13}H_9NSCl^+$, was possible for the m/z 246 fragment ion formed from the m/z 319 precursor ion featured in Fig. 2, based on the average exact mass and RIAs listed in Table 1 and only one composition ($C_4H_{11}N$) was possible for the corresponding 73 Da neutral loss. Their algebraic sum provided the composition ($C_{17}H_{20}N_2S$) enclosed by a rectangle in the three tables in Fig. 2 and thereby rejected the remaining six potential ion compositions. To provide auto-

mation for such analyses using this summation principle, an ion correlation program (ICP) has been developed.

Ion correlation program

An in-house ICP written in QuickBASIC[®] 4.5 rejects numerous compositions, generally leaving only one for the precursor ion, each fragment ion and each neutral loss, by comparing their compositions for consistency. The ICP performs this task in several steps:

1. All possible compositions having at least -0.5 rings and double bonds (RDB) that are consistent with the elemental limits considered, with the exact masses within the mass error limits, and with the RIAs within the RIA tolerance set by the user, are calculated for the precursor and fragment ions and stored for further processing. The precursor ion compositions are calculated first to establish upper elemental limits for the subsequent calculation of the possible fragment ion compositions.
2. All possible neutral loss compositions are calculated based on the mass differences between the precursor ion and all fragment ions. The formulae characterized by an RDB value of no less than -2.0 are saved and stored for further processing.
3. Precursor ion compositions are rejected that cannot be derived by the summation of the number of atoms of each element in a fragment ion-neutral loss pair. This formula-discrimination criterion is applied for each fragment ion exact mass.
4. Fragment ion compositions that do not provide a resulting possible precursor ion when summed with a corresponding neutral loss composition are rejected, as are neutral loss compositions that do not provide a resulting possible precursor ion when summed with a corresponding fragment ion composition.

The ICP requires that ions have at least -0.5 RDB, as calculated by Eqn. (1):²⁵

$$\text{RDB} = (\# \text{ C, Si}) - (0.5 \times \# \text{ H, F, Cl, Br}) + (0.5 \times \# \text{ N, P}) + 1 \quad (1)$$

The $[M+H]^+$ ion for a saturated compound would have -0.5 RDB on the basis of this calculation. Plausible multiple neutral losses to form a fragment ion are assumed to yield no less than -2.0 RDB, as calculated by this equation. For example, successive losses of three water molecules, each having 0 RDB, would provide a total neutral loss formula of H_6O_3 for which the equation provides -2.0 RDB. Equation (1) does not account for the higher valences of S, Se, N, and P in several oxygenated functional groups that are common in organic compounds, such as SO, SO₂, SO₃, NO₂, PO₃, and PO₄. Hence, when enough O atoms are present in an ion, S and Se could have valences of +4 or +6 instead of +2, and N and P a valence of +5 instead of +3. A range of RDB is calculated when O atoms and S, Se, N, or P atoms are present to allow for these higher valences. Valences of +4 and +6 are possible for S and Se when one or two O atoms are available for each S and Se atom, respectively. Likewise, a valence of +5 is possible for N and P when two O atoms in excess of twice the number of S and Se atoms are present for each N and P

Table 1. Exact masses, relative isotopic abundances, and measurement errors for the nine analytes

	Precursor Ion	Fragment Ions			
Exact mass	166.1234 (+0.8)Ex	148.1116 (−0.5)	133.0873 (−1.3)	117.0671 (−2.8)	91
	166.1212 (−1.4)Ex	148.1117 (−0.3)	133.0863 (−2.3)	117.0682 (−1.7)	Below cal.
	166.1199 (−2.7)Ex	148.1121 (+0.1)	133.0874 (−1.2)	117.0692 (−0.7)	range
%1 RIA	12.15 (+4.1%)	11.41 (−1.6%)	9.52 (−8.9%) II	12.10 (+20.4%) II	8.57 (+9.6%)
	12.29 (+5.3%)	11.35 (−2.2%)	9.96 (−4.7%) II	11.11 (+10.5%) II	8.14 (+4.1%)
	12.25 (+5.0%)	11.46 (−1.2%)	9.95 (−4.8%) II	11.13 (+10.7%) II	8.13 (+4.0%)
%2 RIA	0.93 (+0.11)	0.63 (+0.02)	7.69 (+7.20) II	3.66 (3.21) II	0.56 (+0.30)
	0.92 (+0.10)	0.58 (−0.03)	6.83 (+6.34) II	3.03 (2.58) II	0.56 (+0.30)
	0.95 (+0.13)	0.60 (−0.01)	8.30 (+7.81) II	3.06 (2.61) II	0.57 (+0.31)
Averages	166.1215 (−1.1)Ex	148.1118 (−0.3)	133.0870 (−1.6)	117.0681 (−1.7)	91
	12.23 (+4.8%)	11.41 (−1.7%)	9.81 (−6.1%) II	11.45 (13.9%) II	8.28 (+5.9%)
	0.93 (+0.11)	0.60 (−0.01)	7.61 (7.12) II	3.25 (2.80) II	0.56 (+0.30)
Average max. ion abundance	2.9E6	1.5E7	1.7E6	1.6E6	2.2E8
Composition	C ₁₀ H ₁₆ NO	C ₁₀ H ₁₄ N	C ₉ H ₁₁ N	C ₉ H ₉	C ₇ H ₇
Neutral loss		H ₂ O	CH ₅ O	CH ₇ NO	C ₃ H ₉ NO
Exact mass	170.0973 (+0.9)	152.0632 (+1.2)	145.0835 (−5.1)	143.0908 (+5.2)	93
	170.0994 (+2.9)	152.0628 (+0.7)	145.0904 (+1.8)	143.0904 (+4.0)	Below cal.
	170.0984 (+1.9)	152.0610 (−1.1)	145.0937 (+5.1)	143.0919 (+6.3)	range
%1 RIA	13.65 (−0.9%)	16.36 (+22.6%) II	9.90 (−14.3%)	14.44 (+17.5%) II	9.12 (+28.8%) II
	14.09 (+2.3%)	16.49 (+23.6%) II	11.50 (−0.4%)	15.63 (+27.2%) II	8.67 (+22.5%) II
	14.05 (+2.0%)	16.26 (+21.9%) II	10.77 (−6.8%)	15.27 (+24.2%) II	8.43 (+19.1%) II
%2 RIA	0.87 (0)	4.60 (+3.78) II	0.56 (−0.05)	10.80 (+10.11) II	2.37 (+2.16) II
	0.98 (+0.11)	4.66 (+3.84) II	0.57 (−0.04)	10.35 (+9.66) II	1.79 (+1.58) II
	0.95 (+0.08)	4.55 (+3.73) II	0.62 (+0.01)	10.62 (+9.93) II	1.91 (+1.70) II
Averages	170.0983 (+1.9)	152.0623 (+0.3)	145.0892 (+0.6)	143.0910 (+5.5)	93
	13.93 (+1.2)	16.37 (+22.7%) II	10.72 (−7.2%)	15.11 (+23.0%) II	8.74 (+23.4%) II
	0.93 (+0.06)	4.60 (+3.78) II	0.58 (−0.03)	10.59 (+9.90) II	2.02 (+1.81) II
Average max. ion abundance	9.7E5	5.3E5	1.3E4	2.8E4	1.1E7
Composition	C ₁₂ H ₁₂ N	C ₁₂ H ₈	C ₁₀ H ₁₁ N	C ₁₁ H ₁₁	C ₆ H ₇ N
Neutral loss		NH ₄	C ₂ H	CHN	C ₆ H ₅
Exact mass	181.0759 (−0.1)	154.0687 (+3.6)	120.0556 (−12.6)		
	181.0767 (+0.7)	154.0765 (+11.4)	120.0733 (+5.1)		
	181.0784 (+2.4)	154.0788 (+13.7)	120.0593 (−8.9)		
%1 RIA	14.11 (+0.1%)	17.40 (+38.0%) II	9.38 (+9.5%)		
	13.99 (−0.7%)	16.76 (+32.9%) II	9.79 (+14.2%)		
	14.15 (+0.4%)	17.28 (+37.0%) II	7.29 (−14.9%)		
%2 RIA	1.17 (+0.25)	1.23 (+0.50) II	0.69 (+0.37)		
	1.13 (+0.21)	1.40 (+0.67) II	1.03 (+0.71)		
	1.11 (+0.19)	1.18 (+0.45) II	0.80 (+0.48)		
Averages	181.0770 (+1.0)	154.0747 (+9.5)	120.0627 (−5.5)		
	14.08 (−0.0%)	17.15 (+36.0%) II	8.82 (+2.9%)		
	1.14 (+0.22)	1.27 (+0.54) II	0.84 (+0.52)		
Average max. ion abundance	7.5E5	4.2E4	3.5E3		
Composition	C ₁₂ H ₉ N ₂	C ₁₁ H ₈ N	C ₇ H ₈ N ₂		
Neutral loss		CHN	C ₅ H		
Exact mass	182.0090 (−0.3)	166.9858 (+0.0)	123.0126 (−1.1)	109.0075 (−3.2)	103.0410 (−0.7)
	182.0105 (+1.2)	166.9880 (+2.2)	123.0129 (−0.8)	109.0085 (−2.2)	103.0388 (−2.9)
	182.0091 (−0.2)	166.9868 (+1.0)	123.0126 (−1.1)	109.0081 (−2.5)	103.0385 (−3.2)
%1 RIA	10.61 (−2.5%)	9.58 (−1.6%)	8.25 (+5.2%) II	7.65 (+2.3%) II	9.62 (+17.9%) II
	10.72 (−1.5%)	9.62 (−1.2%)	8.04 (+2.6%) II	7.77 (+3.9%) II	9.69 (+18.8%) II
	10.70 (−1.7%)	9.58 (−1.6%)	8.22 (+4.8%) II	7.82 (+4.5%) II	10.03 (+22.9%) II
%2 RIA	9.63 (+2.4%)	9.50 (+2.3%)	4.70 (0) II	4.78 (+2.4%) II	Low ion abundance
	9.79 (+4.1%)	9.46 (+1.8%)	4.74 (+0.9%) II	4.78 (+2.4%) II	Low ion abundance
	9.88 (+5.1%)	9.42 (+1.4%)	4.77 (+1.5%) II	4.90 (+4.9%) II	Low ion abundance
Averages	182.0095 (+0.3)	166.9869 (+1.1)	123.0127 (−1.0)	109.0080 (−2.6)	103.0394 (−2.2)
	10.68 (−1.9%)	9.59 (−1.5%)	8.17 (+4.2%) II	7.75 (+3.6%) II	9.78 (+19.9%)
	9.77 (+3.9%)	9.46 (+1.8%)	4.74 (+0.8%) II	4.82 (+3.2%) II	Low ion abundance
Average max. ion abundance	6.4E6	6.5E6	1.1E6	1.0E6	1.6E5
Composition	C ₈ H ₈ NS ₂	C ₇ H ₅ NS ₂	C ₆ H ₅ NS	C ₆ H ₅ S	C ₇ H ₅ N
Neutral loss		CH ₃	C ₂ H ₃ S	C ₂ H ₃ NS	CH ₃ S ₂

Continues

Table 1. Continued

	Precursor ion	Fragment ions				
Exact mass	192.1382 (−0.1)	119.0481 (−1.0)	109.0810 (−7.6)	91	72	65
	192.1368 (−1.5)	119.0472 (−1.9)	109.0802 (−8.4)	Below cal.	Below cal.	Below cal.
	192.1383 (+0.0)	119.0482 (−0.9)	109.0810 (−7.6)	range	range	range
%1 RIA	13.81 (−0.6%)	8.81 (−1.7%)	7.77 (−5.8%) II	7.70 (−1.5%)	4.05 (+6.6%)	5.40 (−3.4%)
	14.05 (+1.1%)	8.92 (−0.4%)	8.14 (−1.1%) II	7.69 (−1.7%)	3.77 (−0.8%)	5.57 (−0.4%)
	13.86 (−0.3%)	9.03 (+0.8%)	7.98 (−3.3%) II	7.70 (−1.5%)	3.82 (+0.5%)	5.38 (−3.8%)
%2 RIA	1.12 (+2.8%)	0.56 (+0.01)	0.63 (+0.33) II	0.46 (+0.20)	0.26 (+0.01)	0.12 (−0.01)
	1.14 (+4.6%)	0.56 (+0.01)	0.49 (+0.19) II	0.48 (+0.22)	0.36 (+0.11)	0.16 (+0.03)
	1.12 (+2.8%)	0.63 (+0.08)	0.48 (+0.18) II	0.51 (+0.25)	0.26 (+0.01)	0.18 (+0.05)
Averages	192.1378 (−0.5)	119.0478 (−1.3)	109.0807 (−7.9)	91	72	65
	13.91 (+0.0%)	8.92 (−0.4%)	7.96 (−3.5%) II	7.70 (−1.6%)	3.88 (+2.1%)	5.45 (−2.5%)
	1.13 (+3.4%)	0.58 (0.03)	0.53 (+0.23) II	0.48 (+0.22)	0.29 (+0.04)	0.15 (+0.02)
Average max. ion abundance	1.3E6	1.2E6	1.4E4	1.4E8	6.6E6	3.1E7
Composition	C ₁₂ H ₁₈ NO	C ₈ H ₇ O	C ₇ H ₁₁ N	C ₇ H ₇	C ₃ H ₆ NO	C ₅ H ₅
Neutral loss		C ₄ H ₁₁ N	C ₅ H ₇ O	C ₅ H ₁₁ NO	C ₉ H ₁₂	C ₆ H ₁₃ NO
Exact mass	214.0839 (−5.7)	158.0307 (+3.7)	141.0018 (+1.3)	77		
	214.0848 (−4.8)	158.0283 (+1.3)	141.0004 (−0.1)	Below cal.		
	214.0833 (−6.3)	158.0303 (+3.3)	141.0009 (+0.4)	range		
%1 RIA	12.49 (0)	7.84 (−1.5%)	6.89 (−8.7%)	6.55 (−2.1%)		
	12.75 (+2.1%)	7.88 (−1.0%)	6.93 (−8.2%)	6.68 (−0.2%)		
	13.14 (+5.2%)	8.54 (+7.3%)	7.36 (−2.5%)	6.69 (0)		
%2 RIA	5.93 (+6.8%)I	4.77 (−6.6%)	5.69 (+12.0%)	0.54 (+0.35)		
	6.48 (+16.8%)I	4.97 (−2.7%)	5.45 (+7.3%)	0.88 (+0.69)		
	6.74 (+21.4%)I	4.98 (−2.5%)	4.95 (−2.6%)	0.19 (0)		
Averages	214.0840 (−5.6)	158.0298 (+2.7)	141.0010 (+0.6)			
	12.79 (+2.4%)	8.09 (+1.6%)	7.06 (−6.5%)	6.64 (−0.7%)		
	6.38 (+15.0%)I	4.91 (−4.0%)	5.36 (+5.6%)	0.54 (+0.35)		
Average max. ion abundance	2.1E5	2.9E5	2.8E5	1.2E7		
Composition	C ₁₀ H ₁₆ NO ₂ S	C ₆ H ₈ NO ₂ S	C ₆ H ₅ O ₂ S	C ₆ H ₅		
Neutral loss		C ₄ H ₈	C ₄ H ₁₁ N	C ₄ H ₁₁ NO ₂ S		
Exact mass	216.0698 (−8.8)	198.0636 (−4.4)	154.0459 (+4.1)	140.0341 (+7.9)	132.0705 (−10.3)	77
	216.0736 (−5.0)	198.0739 (+5.9)	154.0496 (+7.8)	140.0310 (+4.9)	132.0772 (−3.6)	Below cal.
	216.0718 (−6.8)	198.0706 (+2.6)	154.0447 (+2.9)	140.0337 (+7.6)	132.0871 (+6.3)	range
%1 RIA	9.17 (−21.6%)	11.55 (−0.6%)	14.11 (+51.4%) II	9.63 (+17.6%) II	9.43 (−9.7%) II	9.06 (+35.4%) II
	10.86 (−7.1%)	11.15 (−4.0%)	13.59 (+45.8%) II	10.20 (+24.5%) II	10.50 (+0.6%) II	7.94 (+18.7%) II
	9.71 (−16.9%)	11.23 (−3.4%)	13.62 (+46.1%) II	10.51 (+28.3%) II	10.47 (+0.3%) II	9.88 (+47.7%) II
%2 RIA	35.55 (+7.7%)	31.70 (−3.3%)	33.99 (+5.0%) II	31.61 (−2.0%) II	1.15 (+134.7%) II	3.69 (+3.50) II
	35.58 (+7.8%)	30.90 (−5.8%)	32.79 (+1.3%) II	29.61 (−8.2%) II	1.13 (+130.6%) II	3.12 (+2.93) II
	34.50 (+4.6%)	30.93 (−5.7%)	32.70 (+1.1%) II	32.04 (−0.7%) II	1.05 (+114.3%) II	3.75 (+3.56) II
Averages	216.0717 (−6.9)	198.0694 (+1.3)	154.0467 (+4.9)	140.0329 (+6.8)	132.0783 (−2.5)	77
	9.91 (−15.2%)	11.31 (−2.7%)	13.77 (+47.8%) II	10.11 (+23.5%) II	10.13 (−2.9%) II	8.96 (+33.9%) II
	35.21 (+6.7%)	31.18 (−4.9%)	33.16 (2.5%) II	31.09 (−3.7%) II	1.11 (+126.5%) II	3.52 (+3.33) II
Average max. ion abundance	4.9E5	9.0E4	1.8E5	6.9E4	3.0E4	3.2E6
Composition	C ₁₀ H ₁₅ ClNO ₂	C ₁₀ H ₁₃ ClNO	C ₉ H ₁₁ Cl (C ₈ H ₉ CIN)*	C ₈ H ₉ Cl (C ₇ H ₇ CIN)*	C ₉ H ₁₀ N	C ₆ H ₅
Neutral loss		H ₂ O	CH ₄ NO ₂ (C ₂ H ₆ O ₂)*	C ₂ H ₆ NO ₂ (C ₃ H ₈ O ₂)*	CH ₅ ClO ₂	C ₄ H ₁₀ ClNO ₂
Exact mass	284.9642 (+3.0)	222.9664 (−2.4)	186.9934 (+1.2)	160.9773 (+0.8)	124.9932 (−6.6)	
	284.9639 (+2.7)	222.9659 (−2.9)	186.9980 (+5.8)	160.9816 (+5.1)	124.9926 (−7.2)	
	284.9633 (+2.1)	222.9656 (−3.2)	186.9949 (+2.7)	160.9810 (+4.5)	124.9942 (−5.6)	
%1 RIA	7.26 (+4.3%)	4.79 (+1.7%)	4.47 (−4.9%)	2.40 (−2.4%)	2.42 (−1.2%)	
	7.28 (+4.6%)	4.60 (−2.3%)	4.52 (−3.8%)	2.42 (−1.6%)	2.31 (−5.7%)	
	7.20 (+3.4%)	4.60 (−2.3%)	4.68 (−0.4%)	2.39 (−2.8%)	2.39 (−2.4%)	
%2 RIA	100.72 (+3.9%)	64.07 (−1.2%)	32.56 (−0.9%)	31.92 (−2.7%)	0.81 (−0.01)	
	100.40 (+3.6%)	63.37 (−2.3%)	33.09 (+0.7%)	31.37 (−4.4%)	0.84 (+0.02)	
	98.84 (+2.0%)	62.56 (−3.5%)	33.69 (+2.5%)	31.41 (−4.2%)	0.83 (+0.01)	
Averages	284.9638 (+2.6)	222.9660 (−2.9)	186.9954 (+3.3)	160.9800 (+3.5)	124.9933 (−6.5)	
	7.25 (+4.1%)	4.66 (−1.0%)	4.56 (−3.0%)	2.40 (−2.3%)	2.37 (−3.1%)	
	99.99 (+3.1%)	63.33 (−2.3%)	33.11 (+0.7%)	31.57 (−3.8%)	0.83 (+0.01)	

Continues

Table 1. Continued

	Precursor ion	Fragment ions			
Average max. ion abundance	1.1E6	4.5E5	9.9E4	2.5E5	2.1E5
Composition	C ₆ H ₁₃ Cl ₃ O ₄ P	C ₄ H ₁₀ Cl ₂ O ₄ P	C ₄ H ₉ ClO ₄ P	C ₂ H ₇ ClO ₄ P	C ₂ H ₆ O ₄ P
Neutral loss		C ₂ H ₃ Cl	C ₂ H ₄ Cl ₂	C ₄ H ₆ Cl ₂	C ₄ H ₇ Cl ₃
Exact mass	98.9748 (-9.4) 98.9784 (-5.8) 98.9779 (-6.3)	63 Below cal. range			
%1 RIA	0.19 (-0.02) 0.19 (-0.02) 0.20 (-0.01)	2.41 (+6.6%) 2.35 (+4.0%) 2.42 (+7.1%)			
%2 RIA	0.79 (-0.01) 0.80 (0) 0.79 (-0.01)	35.37 (+10.6%) 35.66 (+11.5%) 36.90 (+15.3%)			
Averages	98.9770 (-7.1) 0.19 (-0.02) 0.79 (-0.01)	63 2.39 (+5.9%) 35.98 (+12.5%)			
Average max. ion abundance	5.3E5	8.7E7			
Composition	H ₄ O ₄ P	C ₂ H ₄ Cl			
Neutral loss	C ₆ H ₉ Cl ₃	C ₄ H ₉ Cl ₂ O ₄ P			
Exact mass	319.0968 (-6.2) Ex 319.0968 (-6.2) Ex 319.0971 (-5.9) Ex	274.0368 (-8.4) 274.0452 (+0.0) 274.0478 (+2.6)	246.0079 (-6.0) 246.0073 (-6.6) 246.0144 (+0.5)	239.0764 (+0.1) 239.0683 (-8.0) 239.0734 (-2.9)	
%1 RIA	19.71 (-4.1%) 20.19 (-1.8%) 19.85 (-3.5%)	18.39 (+2.9%) 18.48 (+3.4%) 18.02 (+0.8%)	15.46 (-1.0%) 15.02 (-3.8%) 15.61 (-0.1%)	20.19 (+12.9%) II 21.03 (+17.6%) II 18.84 (+5.4%) II	
%2 RIA	36.53 (-4.9%) 38.10 (-0.8%) 37.18 (-3.2%)	37.87 (-0.1%) 38.74 (+2.2%) 37.63 (-0.7%)	37.46 (-0.2%) 37.83 (+0.7%) 38.48 (+2.5%)	13.01 (+119.4%) II 14.63 (+146.7%) II 12.57 (+112.0%) II	
Averages	319.0969 (-6.1) Ex 19.92 (-3.1%) 37.27 (-3.0%)	274.0433 (-1.9) 18.30 (+2.3%) 38.08 (+0.4%)	246.0099 (-4.0) 15.36 (-1.6%) 37.92 (+1.0%)	239.0727 (-3.6) 20.02 (+12.0%) II 13.40 (+126.0%) II	
Average max. ion abundance	2.8E6	4.7E4	2.4E5	1.5E5	
Composition	C ₁₇ H ₂₀ CIN ₂ S	C ₁₅ H ₁₃ CINS	C ₁₃ H ₉ CINS	C ₁₅ H ₁₃ NS	
Neutral loss		C ₂ H ₇ N	C ₄ H ₁₁ N	C ₂ H ₇ CIN	
Exact mass	233.0140 (-4.6) 233.0080 (-10.6) 233.0133 (-5.3)	214.0359 (-5.9) 214.0384 (-3.4) 214.0384 (-3.4)	211.0418 (-3.2) 211.0413 (-3.7) 211.0436 (-1.4)	86 Below cal. range	58 Below cal. range
%1 RIA	17.14 (+12.2%) 17.43 (+14.1%) 17.06 (+11.7%)	18.20 (+22.7%) II 18.21 (+22.8%) II 17.91 (+20.8%) II	17.06 (+9.2%) II 17.88 (+14.5%) II 17.67 (+13.1%) II	5.89 (-2.8%) 5.92 (-2.3%) 5.89 (-2.8%)	3.93 (+3.7) 4.05 (+6.9) 4.05 (+6.9)
%2 RIA	37.78 (+0.8%) 38.47 (+2.6%) 38.17 (+1.8%)	32.22 (-2.4%) II 32.38 (-1.9%) II 31.79 (-3.7%) II	33.47 (+500%) II 32.54 (+484%) II 32.76 (+488%) II	0.15 (0) 0.14 (-0.01) 0.15 (0)	0.06 (+0.01) 0.06 (+0.01) 0.06 (+0.01)
Averages	233.0118 (-6.9) 17.21 (+12.7%) 38.14 (+1.7%)	214.0376 (-4.2) 18.11 (+22.1%) II 32.13 (-2.7%) II	211.0422 (-2.8) 17.54 (12.3%) II 32.92 (+491%) II	86 5.90 (-2.6%) 0.15 (-0.00)	58 4.01 (+5.8%) 0.06 (+0.01)
Average max. ion abundance	3.3E4	2.9E5	1.3E5	1.1E8	6.9E7
Composition	C ₁₃ H ₁₀ ClS	C ₁₃ H ₉ CIN	C ₁₃ H ₉ NS	C ₅ H ₁₂ N	C ₃ H ₈ N
Neutral loss	C ₄ H ₁₀ N ₂	C ₄ H ₁₁ NS	C ₄ H ₁₁ CIN	C ₁₂ H ₈ CINS	C ₁₄ H ₁₂ CINS

II The RIA could be distorted by the presence of inherent interferences evident in Fig. 5.

I The RIA could be distorted by the presence of a precursor ion at m/z 216 from the previously eluting compound.

Ex The exact mass was measured using external mass calibration.

*The first composition alone was obtained with an 8 mDa mass error limit, while the composition in parentheses was also found with a 10 mDa error limit and is the correct one. The errors are calculated based on the composition in parentheses.

atom. The upper limit of the range of 3.5 to 5.5 RDB calculated for protonated *n*-butylbenzenesulfonamide accounts for the benzene ring (4 RDB) and SO₂ group (2 RDB) less 0.5 RDB for the attached proton.

The ICP requires the monoisotopic exact mass to be entered for an ion to be considered. In addition, the measured exact masses of the +1 Da ion or +2 Da ion, the %1 RIA, or the %2

RIA can, but need not, be entered. However, RIAs alone cannot be entered.

The RIA error limit entered by the user applies to all RIA values of 1% or more. For RIA values less than 1%, the error limit is automatically set to 0.02 times the entered error limit (e.g., 0.2 RIA % units for a 10% error limit). For instance, consider the RIAs in Table 1 for m/z 166. The measured

a				b			
m/z 319.0969 \pm 7 mmu >1/3 C				m/z 319 <19.92 37.27> \pm 10%			
#	Δm (mmu)	Composition		#	%+1	%+2	Composition
1	-0.9	C8	H20 N2 O9 P	1	18.11	37.96	C14 H28 N4 S CL
2	-3.1	C8	H19 N2 O11	2	18.26	37.99	C14 H14 N5 S CL
3	-4.4	C8	H24 N3 O4 P3	3	18.11	33.53	C14 H32 N6 CL
4	+5.1	C8	H22 N3 O6 P S	4	18.42	38.01	C14 N6 S CL
5	-3.9	C8	H25 N4 O P2 S2	5	18.27	33.56	C14 H18 N7 CL
⋮				⋮			
155	-5.3	C17	H20 O2 P S	101	20.00	38.70	C17 H2 N O2 S CL
156	+4.2	C17	H21 O2 P2	102	19.49	34.37	C17 H18 N O3 CL
157	+3.0	C17	H19 O4 S	103	19.28	34.54	C17 H2 N O4 CL
158	+0.1	C17	H18 N O3 CL	104	19.78	33.83	C17 H21 N2 P CL
159	+6.1	C17	H20 N2 S CL	105	20.56	38.41	C17 H20 N2 S CL
160	+1.2	C17	H14 N5 P	106	20.05	34.08	C17 H36 N2 O CL
161	-5.1	C18	H20 O S CL	107	19.58	33.99	C17 H5 N2 O P CL
162	+4.4	C18	H21 O P CL	108	20.36	38.57	C17 H4 N2 O S CL
163	-1.8	C18	H13 N3 O3	109	19.85	34.24	C17 H20 N2 O2 CL
⋮				⋮			
168	-0.4	C20	H15 O4	150	21.17	34.71	C19 H8 O3 CL
169	+5.6	C20	H17 N O S	151	21.47	34.17	C19 H11 N P CL
170	+2.8	C20	H16 N2 CL	152	21.73	34.42	C19 H26 N O CL
171	+0.9	C21	H11 N4	153	21.53	34.58	C19 H10 N O2 CL
172	+2.3	C23	H13 N O	154	21.89	34.46	C19 H12 N2 O CL
⋮				⋮			
c							
m/z 319.0969 \pm 7 mmu				<19.92 37.27> \pm 10%			
#	Δm (mmu)	%+1	%+2	Composition			
1	-1.3	18.32	33.96	C15 H16 N4 O2 CL			
2	+3.1	19.02	33.69	C16 H19 N3 P CL			
3	-6.5	19.79	38.27	C16 H18 N3 S CL			
4	+0.1	19.49	34.37	C17 H18 N O3 CL			
5	+6.1	20.56	38.41	C17 H20 N2 S CL			
6	+4.4	20.19	34.11	C18 H21 O P CL			
7	-5.1	20.96	38.69	C18 H20 O S CL			

Figure 2. Partial tables of possible compositions: (a) for an m/z 319.0969 ion based on an exact mass error limit of 7 mDa, (b) for a nominal mass 319 ion based on RIA error limits of 10%, and (c) on an m/z 319.0969 ion based on both of these error limits. The measured average exact mass ($N=3$) and measured average RIAs ($N=3$) from Table 1 were entered into a composition generator (PGM); ^{10}C , H, N, O, P, S, and Cl were the elements considered.

average %1 RIA of 12.23% is 4.8% larger than the calculated value of 11.67%, while the measured average %2 RIA of 0.93% is 0.11 RIA % greater (but it is greater by 13.4% on a relative scale) than the calculated value of 0.82%. This approach provides a wider error acceptance for RIAs less than 1% for which low ion abundances and interferences are most detrimental to accurate measurement.

The ICP is limited to considering a total of 50 compositions for each exact mass due to the limited memory accessed by QuickBASIC[®]. When this limit is exceeded the error message 'Too many compositions—remove one element' appears. Removing one element from consideration, or assuming the largest-mass ion is protonated, halves the number of compositions considered. Specifying lower element limits or specific numbers of atoms for particular elements such as S, Cl, or Br based on their isotopic contributions to %2 RIA values also greatly reduces the number of possible composi-

tions before running the ICP. For example, %2RIA values near 5, 10, 15, 20, 32, 37, 64, and 100%, would suggest the presence of: 1S, 2S, 3S, 4S, 1Cl, SCl, 2Cl, or 3Cl (or 1Br) atoms, respectively. Lower limits for the number of C atoms are suggested by the presence of two characteristic aromatic ions. Abundant ions at m/z 77 and 91 observed in product ion mass spectra suggest the presence of at least 6 and 7 C atoms, respectively. If compositions other than C_6H_5 and C_7H_7 were responsible for these ions and fewer than 6 or 7 C atoms were present, no compositions would be found, and this assumption would be proven to be false.

Sources of error in RIA and exact mass measurements

In the absence of interferences, RIAs were accurate to within 5% for the majority of measurements and almost always accurate to within 10%, the RIA error limit initially entered into

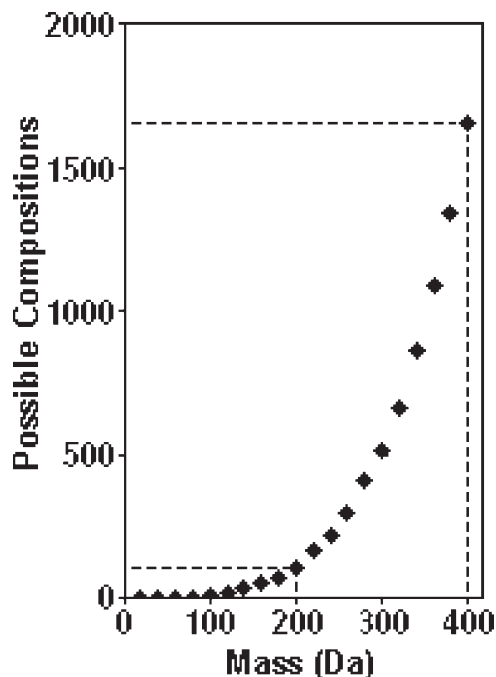


Figure 3. A plot of the number of possible compositions based on a mass error limit of 7 mDa for masses of 20.0000 to 400.0000 Da at 20 Da increments considering only the elements C, H, Cl, N, O, P, and S.

the ICP. For internal calibration, all corrected exact masses were accurate to within 5 mDa for ions with abundances above 5.3×10^5 and to within 10 mDa for abundances greater than to 4.2×10^4 .

Figure 4 illustrates why larger errors in RIA values are expected when mass peaks are observed in the monoisotopic product ion spectra at m/z values -2 , -1 , $+1$, or $+2$ from the m/z of the monoisotopic analyte ion M . The left column (Figs. 4(a), 4(c) and 4(e)) shows three abbreviated monoisotopic product ion spectra and the right column (Figs. 4(b), 4(d) and 4(f)) shows corresponding full-scan mass spectra, which display the isotopic ions of M . In Fig. 4(a) only the monoisotopic ion is drawn; there are no other monoisotopic ions within ± 2 Da. The full-scan spectrum in Fig. 4(b) displays the expected isotopic abundances for the $+1$ and $+2$ ions. In Fig. 4(c) there are monoisotopic ions $+1$ and $+2$ Da higher in mass than the monoisotopic ion. The full scan in Fig. 4(d) illustrates that these $+1$ and $+2$ monoisotopic ion abundances add to the isotopic ion abundances for M to provide inflated $\%1$ RIA and $\%2$ RIA values. In Fig. 4(e), -1 and -2 monoisotopic ions are present. For illustrative purposes, the -2 Da ion contains a Cl atom, and its $\%2$ RIA is 32%, which adds to the ion abundance of the M ion in Fig. 4(f). The -1 Da monoisotopic ion contains no halogen atoms. It contributes its $\%1$ RIA to the M ion as well, and its smaller $\%2$ RIA to the $+1$ isotopic peak of the M ion. The effect of these contributions is to deflate the measured RIAs for the M ion. However, if the -1 Da ion contained a Cl atom, its $\%2$ RIA would inflate the $\%1$ RIA measured for M . The -2 , -1 , $+1$, and $+2$ Da monoisotopic ions are produced from the analyte and are thus 'inherent interferences'. Additional clean-up of an extract or optimization of HPLC conditions would not remove these interferences. Adjustment of the CID

voltage can, however, sometimes reduce their abundance relative to the monoisotopic ion. These inherent interferences are of most concern when small RIAs are measured. A 0.2% interference is sufficient to cause an expected RIA of 1% to fail a 10% error limit. At the other extreme, a 2% $+2$ Da interference would not cause the $\%2$ RIA of 32% expected for one Cl atom to be outside of the same error limit.

A minor source of RIA errors is the variation in natural isotopic abundances.²⁶ The largest errors result from the number of C atoms in a composition. The variation for 10C atoms would be $10 \times 0.03\% = 0.3\%$, which is small relative to the 10% error limit ($0.10 \times 11.1\% = 1.1\%$) usually entered into the ICP.

Precursor ion RIAs are more likely to be distorted than those measured for fragment ions. Any extraneous ions with the same nominal mass but different compositions than the monoisotopic, $+1$ Da, or $+2$ Da ions of the analyte entering Q2 through the 10-Da mass window selected by Q1 would contribute to the precursor ion abundances. Extraneous ions would be fragmented within Q2, but would only distort

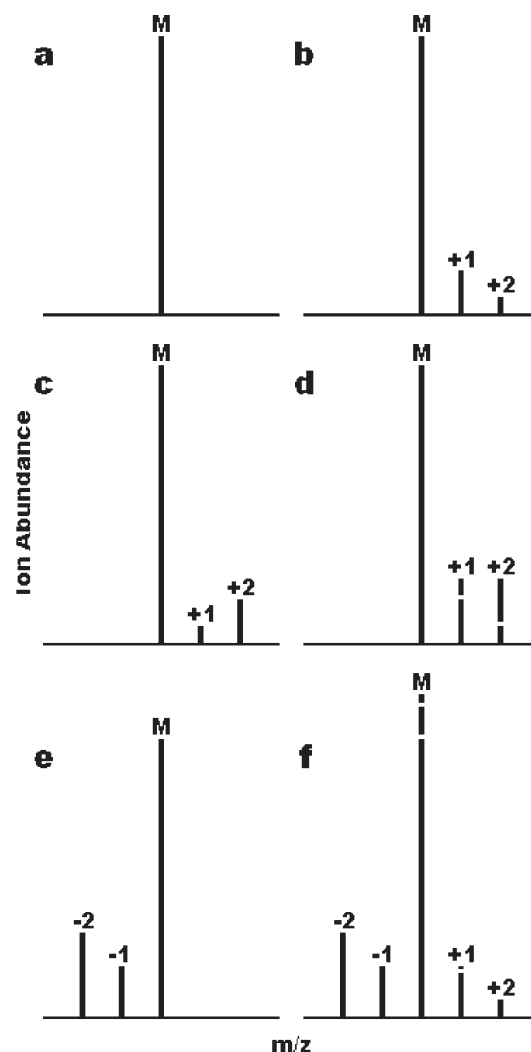


Figure 4. Paired, abbreviated monoisotopic product ion spectra (a, c, and e) and corresponding full-scan mass spectra (b, d, and f). No inherent interferences are illustrated in (a) and (b), $+1$ and $+2$ Da interferences are present in (c) and (d), and -1 and -2 Da interferences are present for (e) and (f).

analyte fragment ion RIAs if the extraneous ion fragments had compositions with the same nominal mass as the monoisotopic, +1 Da or +2 Da fragment ions from the analyte.

Exact mass values are less influenced by inherent interferences. The mass difference between ^{12}C and ^{13}C atoms is 1.00335 Da, and the mass of an H atom is 1.00783 Da. The difference between these values is only 4.48 mDa. If an M^+ ion containing 10 C atoms had the same abundance as an $[\text{M}+\text{H}]^+$ ion, the total observed $[\text{M}+\text{H}]^+$ ion abundance would be $10 \times 0.011 + 1.00 = 1.11$, where the contribution from the M^+ ion with one ^{13}C atom would be $0.11 / 1.11 \times 100\% = 9.9\%$. The weighted average exact mass would be distorted by $(0.11 \times 1.00335 + 1.00 \times 1.00783) / 1.11 - 1.00783 \text{ mDa} = -0.44 \text{ mDa}$, which is small compared to the 10 mDa error limit most often entered into the ICP. The monoisotopic precursor and fragment ion abundances are usually large relative to interferences of the same nominal mass, and their exact masses are measured with sufficient accuracy. The exact masses of the much less abundant +1 and +2 ions would be more distorted by a similar level of a mass interference, but they are not measured.

Choosing inputs for the ICP

One is free to make as many assumptions as are needed to obtain a set of unique ion and neutral loss compositions from the ICP. Suppositions that are incorrect, such as overly restrictive error limits or failure to consider an element present in the molecule, will provide no compositions. The following assumptions were made.

- (i) RIA values based on high maximum ion abundances (1×10^5 or more) for ions greater in mass than 100 Da were more likely to be accurate than values obtained from lower maximum ion abundances or at masses below 100 Da. Because exact masses are less susceptible to alteration by interferences, these restrictions were not applied for exact mass measurements and more exact masses than RIAs were entered into the ICP.
- (ii) An iterative approach was often used. Mass error limits of 10 mDa and RIA error limits of 10% were initially assumed to be adequate for all measurements entered into the ICP. When these generous error limits provided multiple possible compositions for one or more ions or neutral losses, the mass error limit was reduced until a unique composition was found for all ions and neutral losses or until no compositions were found, which indicated that one or more measurement errors exceeded the error limit last entered into the ICP. When no compositions were found with the 10 mDa and 10% error limits, the RIA error limit was increased until compositions were found. Then the mass error limit was reduced, if multiple compositions were listed for one or more ions or neutral losses.
- (iii) The elements considered were C, H, N, O, P and S, unless the measured %2 RIA exceeded 25%, in which case Cl was also considered. One %2 RIA of at least 90% mandated inclusion of Br, as well. If no compositions were found using the ICP, and low %1 RIA values were measured, consideration of additional monoisotopic elements, such as F, I, or As, would be warranted.

- (iv) Initially, no assumption was made concerning whether or not the precursor ion was protonated.
- (v) When too many compositions were generated, elemental limit assumptions were made as discussed above.

These assumptions were employed as measured exact masses and RIAs for the ions formed from the nine analytes were entered into the ICP with the following results.

m/z 166: From Table 1, the average maximum ion abundances for the *m/z* 166 precursor ion and its three highest-mass fragments were large and their masses exceeded 100 Da. Because the -2 Da and -1 Da inherent interferences evident in the abbreviated monoisotopic product ion mass spectrum in Fig. 5(a) indicated that the *m/z* 133 and 117 RIAs might be distorted, they were not entered into the ICP. The four average monoisotopic exact masses and average RIAs for the *m/z* 166 and 148 ions from Table 1 were entered into the ICP with 10 mDa and 10% error limits. The unique compositions for the precursor ion, its three fragment ions, and the corresponding neutral losses in Table 1, were found. Entering the measured values and error limits for each of two of the three data sets provided the same unique compositions. For the third data set, the mass error limit was reduced to 9 mDa to obtain the unique compositions. The mass of the *m/z* 91 ion fell below the calibration range. The calculated %1 RIA for C_7H_7 was 7.82%, which was within 6% of the measured value of 8.28%. The %1 RIAs calculated for the other possible compositions based on the composition of the precursor ion were 7.05% or less.

m/z 170: Only the average maximum ion abundances for *m/z* 170 and 152 exceeded 1×10^5 . The *m/z* 152 RIAs were distorted by the inherent interferences evident in Fig. 5(b). Entering the four average or individual exact masses from Table 1 and the average or individual RIAs for the *m/z* 170 ion into the ICP with error limits of 10 mDa and 10% yielded unique compositions for all four ions and the three neutral losses. Two compositions, $\text{C}_6\text{H}_7\text{N}$ and C_7H_9 , were possible for the *m/z* 93 ion based on the elemental limits provided by the precursor ion. The inherent interferences seen in Fig. 5(b) for *m/z* 93 suggested the measured RIAs were unreliable. Indeed, the values were too high for both compositions; $\text{C}_6\text{H}_7\text{N}^+$ was listed in Table 1 because C_7H_9^+ would probably lose two H atoms to provide the very stable tropylium ion, C_7H_7^+ .

m/z 181: Only the precursor ion abundance exceeded 1×10^5 . No significant inherent interferences were seen in Fig. 5(c) for the *m/z* 181 ion. Entering the three exact masses and RIAs for the *m/z* 181 ion with 10 mDa and 10% error limits provided no compositions for any ion. The small %2 RIA was susceptible to inflation by minor interferences. The same entries were made, but without the %2 RIA value. The unique compositions in Table 1 were then found. For the three data sets, no compositions were found with the 10 mDa error limit; when it was increased to 15 mDa, unique compositions were determined for two of the data sets, while for the third set two compositions were found for each fragment ion. Adding the assumption that the precursor ion was an $[\text{M}+\text{H}]^+$ ion provided unique compositions for the third data set. For the average values, the unique compositions were also found by entering both RIA values for the *m/z* 181 ion and increasing the RIA error limit to 15%. For the individual data sets, mass

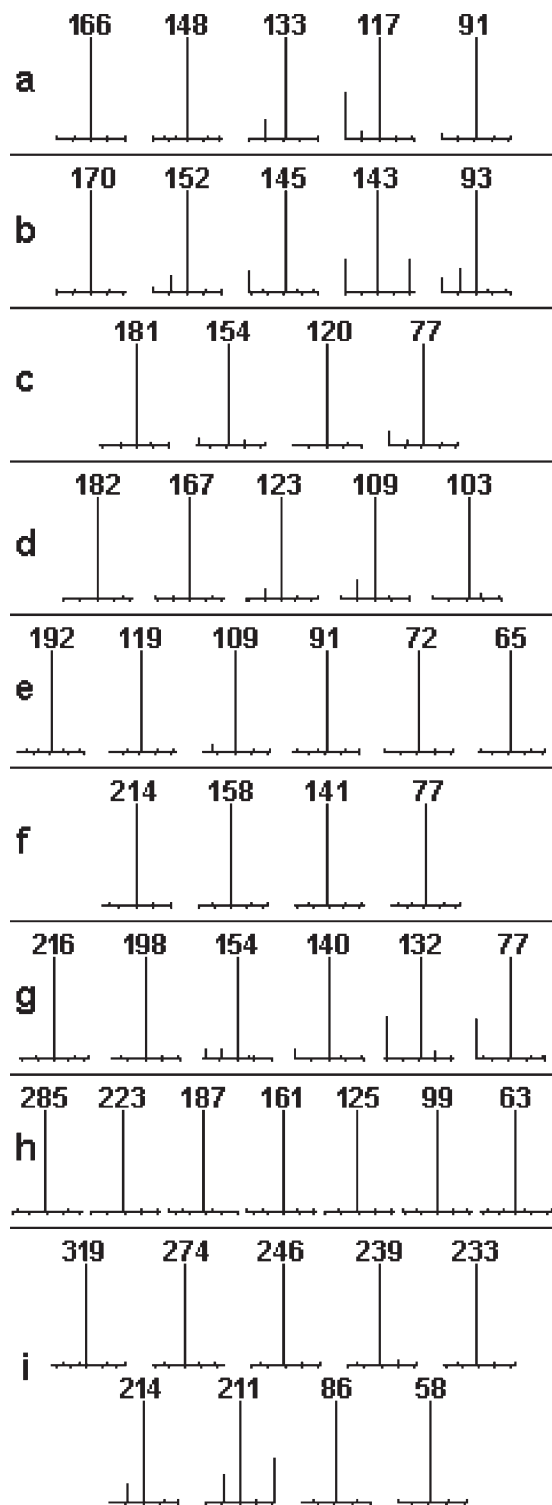


Figure 5. Normalized portions of the monoisotopic product ion mass spectra in Fig. 1 from -2 to $+2$ Da about each ion studied at the CID voltage used to produce each ion.

error limits of 15 mDa and 15% provided unique compositions for two sets, and also for the third set when the same precursor ion assumption was made.

m/z 182: After checking Fig. 5(d) for inherent interferences, the five average exact masses and average RIAs for the *m/z* 182 and 167 ions from Table 1 were entered into the ICP with 10 mDa and 10% error limits. Unique compositions were found for all but the *m/z* 109 ion. Three compositions were

possible for both this ion and its corresponding neutral loss. The mass error was reduced until either unique ions were found for all exact masses, or until no compositions were found because the error limit had become too small for at least one mass measurement. In this case, a 6-mDa error limit provided unique compositions for all ions and neutral losses. These entries provided unique compositions for the averages and for each of the three data sets.

m/z 192: In Fig. 5(e), the *m/z* 192 and 119 ions were free of inherent interferences and had high average maximum ion abundances. The exact masses for the *m/z* 192, 119, and 109 ions, and the RIAs for the *m/z* 192 and 119 ions, were entered into the ICP with 10 mDa and 10% error limits. The unique compositions in Table 1 were obtained for the average values and for each of the three data sets. The *m/z* 91, 72, and 65 ions had high average maximum ion abundances and no inherent interferences were evident for these ions in Fig. 5(e), and hence their measured RIAs were useful for determining their compositions; of the possible compositions based on the elemental limits provided by the precursor ion, the compositions in Table 1 (C_7H_7 , C_3H_6NO , and C_5H_5) had calculated RIAs closest to those measured for the *m/z* 91, 72, and 65 ions, respectively.

m/z 214: The average maximum ion abundances for the compound that provided an *m/z* 214 precursor ion all exceeded 1×10^5 . No inherent interferences were seen in Fig. 5(f) for the *m/z* 214, 158, or 141 ions. No compositions were found by the ICP when the three average exact masses and their corresponding RIAs were entered using 10 mDa and 10% error limits. Inspection of the *m/z* 216 ion chromatogram revealed a large interference, and a small *m/z* 216 chromatographic peak was observed that tracked the *m/z* 214 chromatographic peak. The *m/z* 216 interference was from the compound that eluted 15 s earlier. The same three exact masses, the %1 RIA measured for the *m/z* 214 ion, and the four RIAs for the other two ions, were entered into the ICP using 10 mDa and 10% error limits. Two compositions were found for both the *m/z* 158 ion and its corresponding neutral loss. Making the same entries, but with a mass error limit of 9 mDa, provided the unique compositions in Table 1. For the three data sets, unique compositions were found for the same entries for one data set, with the mass error reduced to 8 mDa for another data set, and with error limits of 7 mDa and 15% and the assumption that the precursor ion was an $[M+H]^+$ ion for the third data set. Alternatively, increasing the RIA error limit to 15% and entering the three average exact masses and three average pairs of RIAs with a mass error limit of 9 mDa provided the same unique compositions. The *m/z* 77 ion was $C_6H_5^+$ based on the elemental limits provided by the precursor ion and the %1 RIA. The %2 RIA was inaccurate, but conclusively indicated that this ion did not contain an S atom.

m/z 216: The ion abundance listed in Table 1 for the *m/z* 216 ion exceeded 1×10^5 and inherent interferences were evident for several of the other ions in Fig. 5(g). The most abundant ion, *m/z* 77, indicated a benzene ring was present, and the %2 RIAs for four ions of 31 to 35% indicated the presence of a Cl atom. The average exact masses of the five ions and the average RIAs for the *m/z* 216 ion were entered into the ICP with error limits of 8 mDa and 20%. At least six atoms of C and one atom of Cl were assumed to be present. Unique compositions were obtained for all ions and neutral losses.

The individual data sets each provided unique compositions except for one fragment ion and its neutral loss. One data set yielded two compositions each for the m/z 140 ion and its neutral loss with error limits of 8 mDa and 20%; another data set found two compositions each for the m/z 132 ion and its neutral loss with error limits of 11 mDa and 20%; and the third data set provided two compositions each for the m/z 132 ion and its neutral loss with error limits of 11 mDa and 25% and assuming a $[M+H]^+$ precursor ion.

m/z 285: No inherent interferences were seen in Fig. 5(h). All six average exact masses and average pairs of RIAs were entered into the ICP using the 10 mDa and 10% error limits. The unique compositions in Table 1 were found. Unique compositions were also found with the same entries for each of the three data sets. Both Cl and Br were included as possible elements, since the %2 RIA of the precursor was 100%. The same entries were made again, but without considering P as a possible element. As expected, no compositions were found. The m/z 63 ion was determined to be $C_2H_4Cl^+$ based on its RIAs and the elemental limits provided by the precursor ion.

m/z 319: In Fig. 5(i), inherent interferences for the three highest-mass ions were insignificant, but the ion abundance of the m/z 274 ion was low. The seven average exact masses and average %RIA values for the m/z 319 and 246 ions in Table 1 were entered into the ICP with error limits of 7 mDa and 10%, and the assumption was made that one Cl atom was present in the precursor ion. The unique ion and neutral loss compositions in Table 1 were listed by the ICP. With the same error limits, one data set provided unique ion compositions except for the m/z 214 ion and its corresponding neutral loss, for which there were two compositions each. A second data set required a 9-mDa mass error and provided two compositions each for the m/z 274 ion and its neutral loss. The third data set required a mass error of 11 mDa, which provided up to four compositions for all ions and their neutral losses except for the m/z 319 and 274 ions, which still provided unique compositions.

Synergy

These examples illustrate that entering RIAs for one or two ions in addition to the exact masses for the precursor and numerous fragment ions is usually sufficient to provide unique ion compositions for the ions and neutral losses. Greatly limiting the possible compositions for an ion by entering the ion's RIAs into the ICP also imposes similar restrictions on the possible compositions for its related ions. For the m/z 182 precursor ion, entering the five average exact masses with a mass error limit of 6 mDa provided 14 compositions for the precursor ion, 14, 13, 11, and 5 compositions for the fragment ions, and 1, 4, 5, and 6 compositions for their corresponding neutral losses. Using the same mass error limit and including the average RIAs for the precursor ion (m/z 182) or the largest fragment ion (m/z 167) with an RIA error limit of 10% provided unique compositions for all five ions and their corresponding neutral losses. After adding the assumption that the precursor ion was an $[M+H]^+$ ion, entering the average RIAs for either the m/z 123 or 109 ion also provided unique compositions. This example clearly illustrated that the discriminating power of considering both exact

masses and RIAs for an ion was extended to related ions by using the ICP. This approach compensated for the distortion of measured RIAs when inherent interferences were present for some of the fragment ions produced from an analyte. Suspect RIAs were not entered.

Identifying compounds from ion and neutral loss compositions

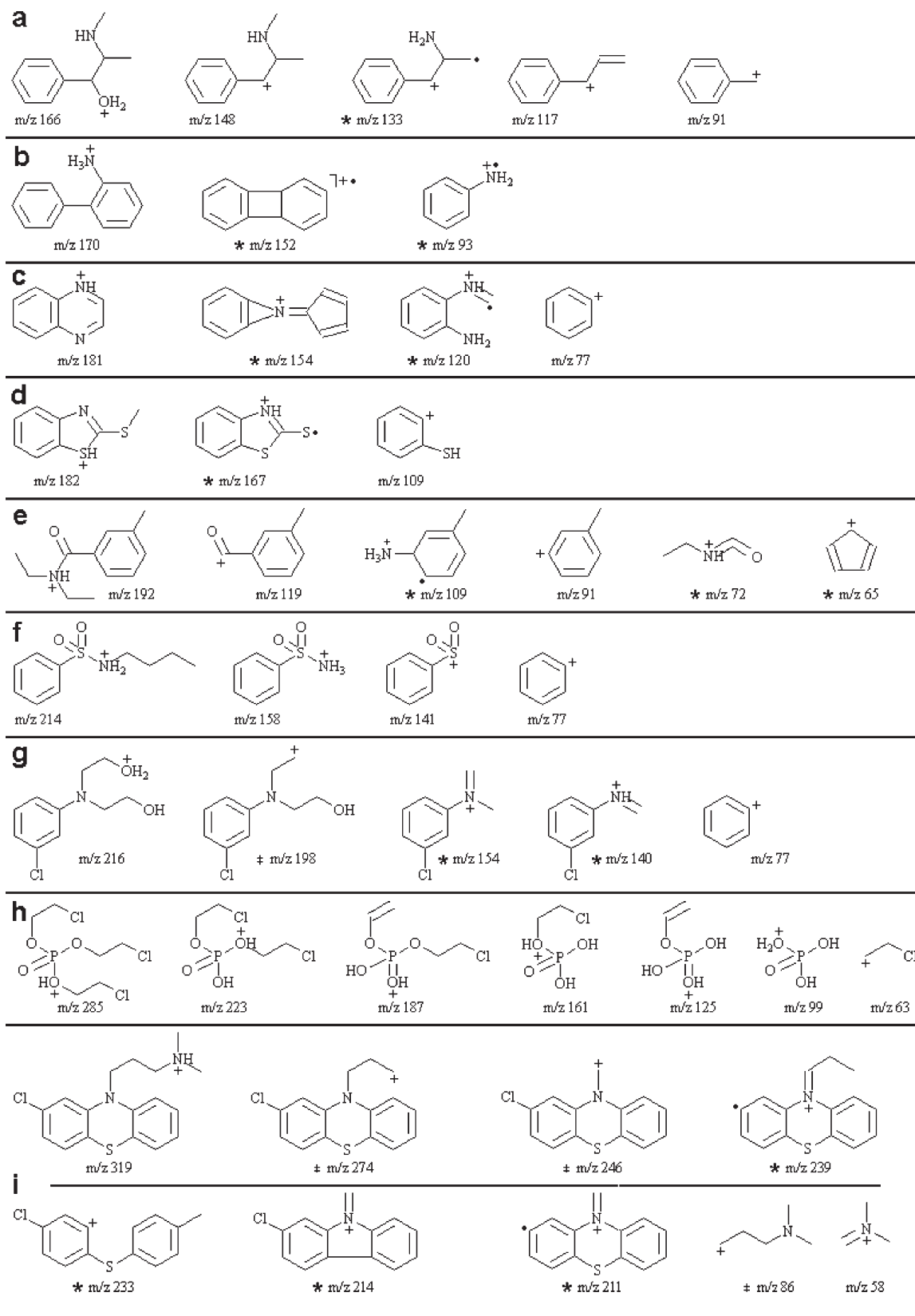
Commercial libraries of APCI (or ESI) mass spectra are not available for comparisons with analyte mass spectra. A compound's identity must be deduced from its precursor ion composition which usually corresponds to a number of possible isomers, and from structural details provided by fragment ion and neutral loss compositions. Fragment ions formed at low CID voltages generally result from cleavage of single bonds and are most useful for this purpose. In addition, the appearance of abundant m/z 77 or 91 ions at higher CID voltages indicates the presence of a benzene ring or an alkylated benzene ring.

There is a strong correlation among compounds used commercially, compounds found in the environment, the number of literature references for a compound, compounds available in chemical catalogs, and compounds in laboratories' chemical inventories. Hence, the chemical literature provides the means to tentatively identify most compounds for which the ion and neutral loss compositions have been determined. SciFinder[®] 27 was used to examine the known structures for the neutral analyte molecules corresponding to the (protonated) precursor ions and to determine the number of literature references for each isomer.

After the most highly referenced structures had been located, the fragment ions and neutral losses were compared with the isomeric structures to choose a tentative identification. Figure 6 shows precursor and fragment ion structures for many of the ions investigated. The majority of these structures were predicted and drawn by the Thermo Finnigan Mass Frontier[®] 3.0 ion fragmentation program. A mass spectral interpretation expert provided the additional structures. For some ions, multiple structures were possible. However, only one plausible structure is required to provide assurance that an ion could be formed from a protonated candidate molecule.

After an analyte's identity is hypothesized to be one isomer or one of a few isomers, those candidate isomers that are commercially available could be purchased to compare their product ion mass spectra at different CID voltages and their retention times with those of the analyte to confirm the identity of the compound. If a preponderance of evidence were desired, the exact masses and RIAs could be measured for the ions produced from the correct standard as well as from the analyte to verify that the ions and neutral losses have the same compositions.

m/z 166 ($C_{10}H_{15}NO$): The low aromaticity (4 RDB) of this composition is consistent with the cleavage of single bonds at low CID voltage reflected in Fig. 1(a). The structure of pseudoephedrine, a decongestant, was cited by 5974 references, while that of a diastereomer was cited by 1626 references. Fewer than 550 references were associated with several other structures. Several phenols and a methoxy compound would be unlikely to yield the observed loss of a



* This structure was not predicted by the software.

‡ The software predicted a primary carbonium ion instead of a quaternary ammonium ion.

Figure 6. Ion structures predicted by the Mass Frontier[®] fragmentation prediction software (Thermo Finnigan) for the ions studied.

water molecule. Three fragment ions with the compositions listed in Table 1 were predicted in Fig. 6(a). If available, both diastereomers would be purchased and tested.

m/z 170 (C₁₂H₁₁N): The high aromaticity of this composition (8 RDB) was reflected by the difficulty of producing fragment ions from the stable *m/z* 152 ion in Fig. 1(b). The loss of NH₃ and NH₄ as (NH₃+H)⁺ indicated the presence of an amino group. We have observed similar losses for benzidine. Only 832 references were indicated for 2-aminobiphenyl, while 1729 references were found for 4-aminobiphenyl and 8560 for diphenylamine. Less than 350 references were found for several compounds containing a pyridine ring. The fragment prediction software provided no structure for the *m/z* 152 ion. If available, these three compounds would be purchased with the expectation that one of the aminobiphenyls would be the correct isomer.

m/z 181 (C₁₂H₈N₂): Again, high aromaticity (10 RDB) resulted in difficult formation of fragment ions, as seen in Fig. 1(c). The structure of phenazine, a chemical intermediate for pharmaceuticals, dyes, and pesticides, garnered 1631 citations, but *o*-phenanthroline amassed 8483 references. Several other N-substituted phenanthrene compounds each provided fewer than 400 citations. The fragment prediction software predicted only the C₆H₅⁺ fragment ion from the protonated phenazine structure in Fig. 6(c). To identify this compound, both phenazine and *o*-phenanthroline would be purchased.

m/z 182 (C₈H₇NS₂): Six RDBs and formation of only one fragment ion at a low CID voltage by loss of a methyl group in Fig. 1(d) suggested aromaticity beyond a benzene ring. The structure for 2-(methylthio)benzothiazole involved in rubber manufacture provided 357 references. The structure for 3-methylbenzothiazole-3-thione with the methyl group attached to the N atom had 149 citations. All other structures had fewer than 50 references. The *m/z* 109 ion predicted in Fig. 6(d) had the correct composition. Both compounds would be purchased.

m/z 192 (C₁₂H₁₇NO): Five RDBs and an *m/z* 91 fragment ion indicated an alkyl benzene ring with an additional double bond in the molecule. The structure for *N,N*-diethyl-3-methylbenzamide (DEET), an insect repellent, provided 1174 references, far more than for any others. The two predicted ions in Fig. 6(e) have the compositions determined in Table 1. This single compound would be purchased.

m/z 214 (C₁₀H₁₆NO₂S): The *m/z* 77 ion indicated the molecule contained a benzene ring. There were 4 to 6 RDB depending on the valence of the S atom. Three facile single-bond cleavages were evident in the -12 V CID product ion mass spectrum in Fig. 1(f). Assuming stepwise losses, a butyl group was lost, followed by losses of NH₃ and SO₂. The protonated structure of the plasticizer *n*-butylbenzenesulfonamide in Fig. 6(f) could yield these ions and returned 316 citations. The tert-butyl isomer had 81 references. Related structures provided fewer references and several lacked a butyl group. If available, both isomers would be purchased.

m/z 216 (C₁₀H₁₄ClNO₂): With 4 to 5 RDB, depending on the valence of the N atom, and an *m/z* 77 ion, this compound had a benzene ring and possibly an additional double bond. The precursor ion readily lost H₂O, suggesting an alcohol. The structures of *N*-(3-chloro)-2,2'-iminodiethanol and the

4-chloro and 2-chloro isomers were accompanied by 90, 13, and 7 references, respectively. A structure with two methoxy groups, unlikely to lose H₂O, had 26 references. Structures with the compositions in Table 1 were *not* predicted for two of the four fragment ions shown in Fig. 6(g). Returning to the ICP, the five average exact masses and average RIAs for the *m/z* 216 ion in Table 1 were entered with error limits of 10 mDa (rather than the 8 mDa limit used earlier) and 20% along with the assumption that the *m/z* 216 ion was an [M+H]⁺ ion. An additional composition was then found for each of the *m/z* 154 and 140 ions and their corresponding neutral losses. These compositions, shown in parentheses in Table 1, were those predicted in Fig. 6(g). The errors in Table 1 were calculated based on these compositions. For this one case out of nine, the strategy of tightening error limits until one composition remained for each fragment ion led to two erroneous fragment ion compositions. Even so, the precursor ion composition was still correct and using SciFinder[®] provided the correct compound as the most likely candidate. The three closely related isomers would be purchased, if available.

m/z 285 (C₆H₁₂Cl₃O₄P): With 0 to 1 RDB, depending on the valence of the P atom, this molecule had no aromaticity. Facile cleavage of several single bonds at a low CID voltage was seen in Fig. 1(h). The *m/z* 99 ion (H₄PO₄⁺) is characteristic of organophosphates, which accounted for the one possible double bond. The structure of tris(2-chloroethyl)phosphate, a flame retardant, garnered 1223 references, many more than all the others. Two structures with the phosphate core and with three Cl atoms on a terminal C atom would not provide the observed fragment ions. All of the fragment ion compositions determined were accounted for in Fig. 6(h). Tris(2-chloroethyl)phosphate would be purchased.

m/z 319 (C₁₇H₁₉ClN₂S): Despite a high degree of aromaticity with 9 RDB, *m/z* 86 and 58 fragment ions appeared at the intermediate CID voltage in Fig. 1(i) and suggested the presence of at least one attached chain of atoms. The structure of chlorpromazine, a sedative, tallied 13 843 references, while fewer than 100 were listed for each of the other structures. The fragment-prediction software yielded four of the eight observed ions with the compositions determined as illustrated in Fig. 6(i). Chlorpromazine hydrochloride would be purchased.

This strategy would be less effective for identifying byproducts, transformation products, and emerging contaminants²⁸ not described in the chemical literature.

Future work

This work has demonstrated that the ICP can provide unique ion and neutral loss compositions essential for reaching tentative identifications of analytes. However, it is written in QuickBASIC, which has memory limitations that make its use less convenient and which is not readily available. Future work will include translating the ICP into Visual Basic and automated importing of ASCII data files containing exact masses and mass profile heights and areas into the program for automated processing. The program will then be suitable for use on modern data systems.

CONCLUSIONS

Compared with use of a double-focusing mass spectrometer, the Thermo Finnigan TSQ Quantum Ultra AM[®] triple-quad-

rupole mass spectrometer (AM3QMS) provided much simpler data acquisition methods and required fewer experiments to measure exact masses and RIAs with sufficient accuracy to determine elemental compositions of protonated molecules. Three scan modes were used in addition to routine full scanning, which was used to determine HPLC retention times of analytes. Monoisotopic precursor ions were isolated and fragmented to provide monoisotopic product ion spectra. Fragment ions were selected for study, and interferences with RIA determinations within 2 Da of the fragment ion masses were noted in these spectra. Then, exact masses were measured for up to 12 ions (seven analyte ions and five calibration ions) by SRM during each scan event. Similarly, nine ion abundances (the monoisotopic ion and its +1 and +2 isotopic ions for three fragment ions) were recorded for RIA measurements.

For 40 ions formed from nine analytes, mass accuracies within 5 and 10 mDa were obtained for average maximum ion abundances that exceeded 5.3×10^5 and 4.2×10^4 , respectively. Absent of interferences, the majority of RIAs obtained were accurate to within 5%, and 134 of 141 were accurate to within 10% for abundances greater than 1×10^4 and masses greater than 98 Da. These error limits, and the ability to measure exact masses or RIAs for fragment ions as well as the precursor ion during single data acquisitions, efficiently provided the data needed to determine unique ion and neutral loss compositions for all ions produced from eight of nine simulated unknowns.

Exact mass measurements were not distorted by interferences, while RIA measurements often were. Use of an ion correlation program (ICP) into which the measured triplicate averages of exact masses for the precursor and fragment ions produced from a compound were entered, in addition to only one or two pairs of average %1 RIA and %2 RIA values, provided unique compositions for all ions studied. Initially, when using the ICP, error limits of 10 mDa and 10% were entered, and the elements C, H, N, O, P, and S were considered. When necessary, different or additional assumptions were made concerning (i) mass and RIA error limits, (ii) the elements and elemental limits considered, (iii) whether or not the precursor ion was an $[M+H]^+$ ion, and (iv) whether gross observation of %RIAs or nominal mass ions provided limits for the number of atoms of any elements. Assumptions were made iteratively until a set of unique ion compositions was obtained for each ion and neutral loss, or until this goal was recognized as unobtainable. For the 27 single sets of data, this goal was met 21 times. However, for three data sets for one compound, the unique compositions found for two fragment ions were incorrect. Even so, the unique composition of the precursor ion was provided by every data set. Hence, the erroneous fragment ion compositions were later revealed and an increase in the mass error limit provided an additional composition for each of the two ions that was correct.

SciFinder[®] was used to provide known structures for the neutral molecules corresponding to the $[M+H]^+$ ion compositions and the number of literature citations for each one. Thermo Finnigan Mass Frontier[®] 3.0 fragment prediction software provided fragment ion structures consistent with many of the ion compositions determined. These tools narrowed identities of each of the simulated unknowns to

between one and three possible isomers, which would be purchased, if available, had these analytes been found in environmental extracts.

Used together, the AM3QMS, ICP, SciFinder[®], and Mass Frontier[®] software are expected to be powerful tools for identifying environmental pollutants that produce APCI (or ESI) mass spectra.

REFERENCES

- 1990 HPV Challenge Program Chemical List, U.S. EPA Office of Pollution Prevention and Toxics (Revised May 28, 2004). Available: http://www.epa.gov/opptintr/chemrtk/hpv_1990.pdf.
- Endocrine Disruptor Screening Program, U.S. EPA Office of Science Coordination and Policy. Available: <http://www.epa.gov/scipoly/oscpendo/>.
- Grange AH, Donnelly JR, Sovocool GW, Brumley WC. *Anal. Chem.* 1996; **68**: 553.
- Grange AH, Brumley WC. *J. Am. Soc. Mass Spectrom.* 1997; **8**: 170.
- Grange AH, Brumley WC. *LC-GC* 1996; **14**: 978.
- Grange AH, Sovocool GW, Donnelly JR, Genicola FA, Gurka DF. *Rapid Commun. Mass Spectrom.* 1998; **12**: 1161.
- Snyder SA, Kelly KL, Grange AH, Sovocool GW, Snyder EM, Giesy JP. In *Pharmaceuticals and Personal Care Products in the Environment: Scientific and Regulatory Issues*, Daughton CG, Jones-Lepp T (eds). Symposium Series 791, American Chemical Society: Washington, DC, 2001; 116–141.
- Grange AH, Thomas PM, Solomon M, Sovocool GW. *Proc. 51st ASMS Conf. Mass Spectrometry and Allied Topics*, Montreal, Ontario, 2003; 6/2-6/6. Available: <http://www.epa.gov/nerlesd1/chemistry/ice/sa.htm>.
- Grange AH, Sovocool GW. *LC-GC* 2003; **21**: 1062.
- Grange AH, Genicola FA, Sovocool GW. *Rapid Commun. Mass Spectrom.* 2002; **16**: 2356.
- NIST/EPA/NIH Mass Spectral Library with Search Program, version NIST '02, Standard Reference Data Program, National Institute of Standards and Technology: Gaithersburg, MD 20899, 2002.
- Wiley Registry of Mass Spectra (6th edn). Palisade Corp.: Newfield, NY (Wiley).
- Hogenboom AC, Niessen WMA, Little D, Brinkman UATH. *Rapid Commun. Mass Spectrom.* 1999; **13**: 125.
- Hsu CS, Green M. *Rapid Commun. Mass Spectrom.* 2001; **15**: 236.
- Bobeldijk I, Vissers JPC, Kearney G, Major H, van Leerdam JA. *J. Chromatog. A* 2001; **929**: 63.
- Palmer ME, Clench MR, Tetler LW, Little DR. *Rapid Commun. Mass Spectrom.* 1999; **13**: 256.
- Maizels M, Budde WL. *Anal. Chem.* 2001; **73**: 5436.
- Jiang L, Moini M. *Anal. Chem.* 2000; **72**: 20.
- Wolff JC, Eckers C, Sage AB, Giles K, Bateman R. *Anal. Chem.* 2001; **73**: 2605.
- Eckers C, Wolff JC, Haskins NJ, Sage AB, Giles K, Bateman R. *Anal. Chem.* 2000; **72**: 3683.
- Zhang H, Heinig K, Henion J. *J. Mass Spectrom.* 2000; **35**: 423.
- Grange AH, Osemwengie L, Brilis G, Sovocool GW. *Int. J. Environ. Forensics* 2001; **2**: 61.
- Grange AH, Donnelly JR, Brumley WC, Billets S, Sovocool GW. *Anal. Chem.* 1994; **66**: 4416–4421.
- Wershaw RL, Ruterford DW, Rostad CE, Garbarino J, Ferrer I, Kennedy KR, Momplaisir GM, Grange AH. *Talanta* 2003; **59**: 1219.
- McLafferty FW, Turecek F. *Interpretation of Mass Spectra* (4th edn). University Science Books: Mill Valley, CA, 1993; 28.
- Lide DR (ed). *Handbook of Chemistry and Physics* (74th edn). CRC Press: Boca Raton, 1994; 1-110–1-111.
- Chemical Abstract Services, American Chemical Society: Columbus, OH. Available: <http://www.cas.org/SCIFINDER/scicover2.html>.
- Daughton CG. *Environ. Impact Assess. Rev.* 2004; **24**: 711. Available: <http://epa.gov/nerlesd1/chemistry/pharma/images/EIAR.pdf>.